Reproducible Copy

N77-33969

AS&E

American Science and Engineering, Inc.
955 Massachusetts Avenue
Cambridge, Massachusetts 02139
617-868-1600

AUGUST 1977

ASE-4173

FINAL REPORT

UPGRADING AND TESTING PROGRAM FOR NARROW BAND HIGH RESOLUTION PLANETARY IR IMAGING SPECTROMETER

PREPARED BY

R.B. WATTSON AND S. RAPPAPORT

CONTRACTS NASW-2883 AND NASW-3066

PREPARED FOR

OFFICE OF SPACE SCIENCES
DIVISION OF PLANETARY PROGRAMS
NATIONAL AERONAUTICS
AND SPACE ADMINISTRATION
WASHINGTON, D.C 20546

ASE-4173

Final Report

UPGRADING AND TESTING PROGRAM FOR NARROW BAND HIGH RESOLUTION PLANETARY IR IMAGING SPECTROMETER

Contracts NASW-2883 and NASW-3066

Prepared by:

Richard B. Wattson and Saul Rappaport
American Science and Engineering, Inc.
955 Massachusetts Avenue
Cambridge, Massachusetts 02139

Prepared for:

Office of Space Sciences
Division of Planetary Programs
National Aeronautics and Space Administration
Washington, D.C. 20546

Submitted by:

Richard B. Wattson

Richard B. Wattson
Project Scientist

Approved by:

A C Vallas

Arthur C. Vallas
Vice President

August 1977

CONTENTS

LIST OF ILLUSTRATIONS

LIST OF ILLUSTRATIONS - CONT.

LIST OF TABLES

1.0 INTRODUCTION

This final report consists of the description of upgrading of an imaging spectrometer intended primarily for observations of the outer planets. The upgrading was performed by American Science and Engineering, Inc. for NASA. The imaging spectrometer utilizes an acoustically tuned optical filter (ATOF) and a charge coupled device (CCD) television camera. The technique that the instrument represents allows for the efficient, simultaneous acquisition of data combining both high spatial resolution of an entire planet and moderately high spectral resolution. The instrument has been used to observe Saturn and Jupiter (Wattson et al, 1976), but aberrations caused by the ATOF severely limited the spatial resolution. The upgrading procedure has improved the imaging spectrometer's spatial resolution and sensitivity.

The ATOF (Harris et al, 1970) has characteristics similar to those of an interference filter except that it is tunable. The filter utilizes a pair of Glan-Thompson Calcite polarizers between which is placed a birefringent $CaMoO_4$ crystal. Acoustic waves, propagated through the crystal, interact with the incoming polarized light beam in such a way that only a narrow range of wavelengths, related to the acoustic frequency, are Bragg scattered into the other polarization state and thus are transmitted by the polarizing analyzer.

The CCD camera is essentially an intrinsic silicon 100 x 100 array of sensors. The sensors exhibit better spatial and photometric reproducibility than vidicon cameras. The charge pattern resulting from the image is read out of the array by passive CCD shift registers in TV sequential format. The data output of the

television camera is a 100 x 100 array of 12 bit numbers which are processed by a dedicated mini-computer system, stored on digital tape and displayed on a digital television system.

The upgraded imaging spectrometer has a spatial resolving power of ~ 1 arc second, as defined by an f/7 beam at the CCD position and it has this resolution over the 50 arc second field of view. The instrument has less vignetting than the original spectrometer and a sensitivity 4 times greater. The spectral resolution of 15 Å over the wavelength interval 6500 Å - 11,000 Å is unchanged. Mechanical utility has been increased by the use of a honeycomb optical table, mechanically rigid yet adjustable optical component mounts, and a camera focus translation stage. The upgraded instrument has been used to observe Venus and Saturn at Harvard's 61" reflector. Due to the limited "seeing" conditions at the site, only the Venus data were of acceptable quality. A simulated image of Saturn taken at the site will be shown.

The present instrument is capable of observations of Jupiter, Saturn, Venus and Mars. At the present time, advances in transducers would allow a larger tunable filter and one with less reflection loss. More sensitive CCD cameras are now available as well. It may thus be possible to observe all of the outer planets as well as the sodium cloud of Io and the emission distribution of planetary nebulae with our technique. At 5 μm, the present availability of an Indium Antiminide, 32 x 32 CID array and a Thallium Arsenic Selenide ATOF would allow the observation of spectral features deep in the atmosphere of Jupiter. Hence we believe that this technique has considerable value beyond the specific observations included herein.

REFERENCES - SECTION 1.0

1. Harris, S.E., Nieh, S.T.K. and Feigelson, R.S. (1970). Appl. Phys. Lett. 17, 223.

2. Wattson, R.B., Rappaport, S.A. and Frederick, E.E. (1976) Icarus 27, 417.

2.0 THE UPGRADED INSTRUMENT

In this section we show laboratory simulated images, CCD sensitivity and the final mechanical configuration adopted for the instrument. The imaging spectrometer is shown in Fig. 1.

2.1 Optical

The internal configuration of the ATOF has a second piece of $CaMoO_4$ (the birefringent acousto-optic material used in the filter) separated by a small air gap at 28^o to the axis to re-direct the light from the first piece of $CaMoO_4$ parallel to the original beam. This causes astigmatism and coma due to the extreme tangentiality of light rays as they pass through the air gap. To correct for these effects a simple cylindrical lens was previously used; however the coma resulting from the air gap was not effectively cancelled out. Hence a large blur (5 arc sec) was observed in the final planetary images. The correction system was redesigned according to the results of a ray tracing analysis. The optics of the imaging spectrometer include:

An achromatic doublet to relay the image from the focus of the Cassegrainian telescope into the ATOF, an achromatic triplet after the ATOF to relay the second image onto the CCD detector and an achromatic cylindrical lens tilted with respect to the optical axis by 12^o. The cylindrical nature of the last lens corrects the astigmatism, which was found to be as much as 100mm axially, and tilting of the cylindrical lens allows its off-axis aberrations to compensate for the extreme coma introduced by the 28^o air gap (in a material with critical angle 30^o). The above optical configuration is shown in Fig. 2. The drawing has a reduced scale, however the relative size and spacings of the optical elements are correct.

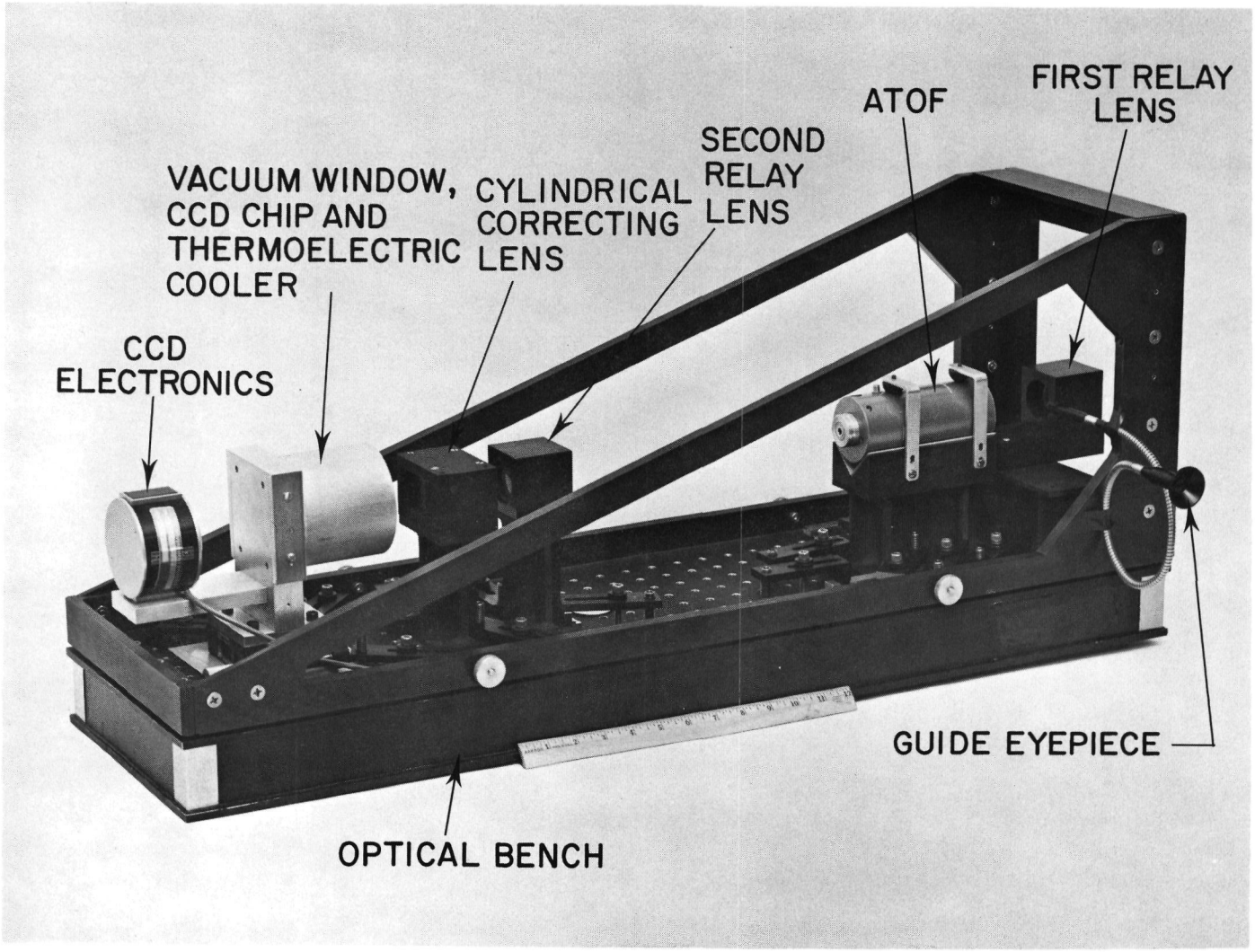

CY-160

Figure 2-1 Imaging Spectrometer

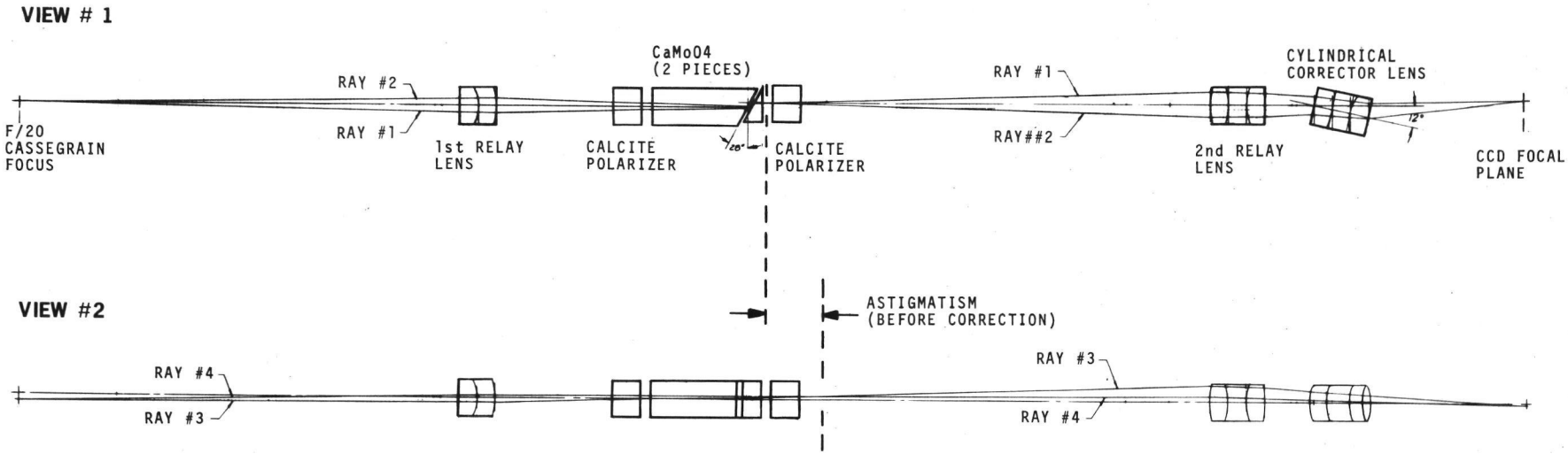

Fig. 2-2. Optical Configuration of the Imagining Spectrometer

D-226

The final optical design was checked for blur circle at a number of points in the field of view and for three chosen wavelengths. Except for a small part of the right side of the field, all blur circles were equal to or less than 0.7 arc seconds FWHM.

Lenses with the above design have been fabricated and aligned in the instrument with the ATOF as an integral part of the optical train. Laboratory test results are shown in Figures 3-5 and Table I. The photographs were taken with an orange filter to produce nearly monochromatic light at a wavelength highly visible and close to the short wavelength cutoff of the correcting optics. Visual inspection of simulated Jupiter and Saturn images indicated better than one arc second spatial resolution. The images in Figures 3 and 4 were produced by an incandescent bulb, ground glass screen, orange filter and 35mm slides of 200" Mt. Palomar telescope pictures. These pictures were taken from Kuiper's Planets and Satellites. The plate scale of the slide images was carefully chosen to simulate the actual sizes of the planets as they would appear at the Cassegrain focus of the Harvard 61" telescope. A focal length of 1200 inches is assumed for the Harvard Reflector (61 inch diameter at f/20).

In addition, a TV test chart, with known calibration (arc seconds on the sky per line pair) is shown in Figure 5. The finest resolved group of bars corresponds to 0.6 arc seconds. While the MTF is significantly reduced at the last group, especially in the horizontal direction, the bars are still discernible in the photograph. Visually obtained resolutions for five parts of the field of view and for both horizontal and vertical bars (vertical and horizontal resolution respectively) are shown in Table I. Thus we have documented qualitatively the kind of planetary images attainable with a still atmosphere and quantitatively the actual

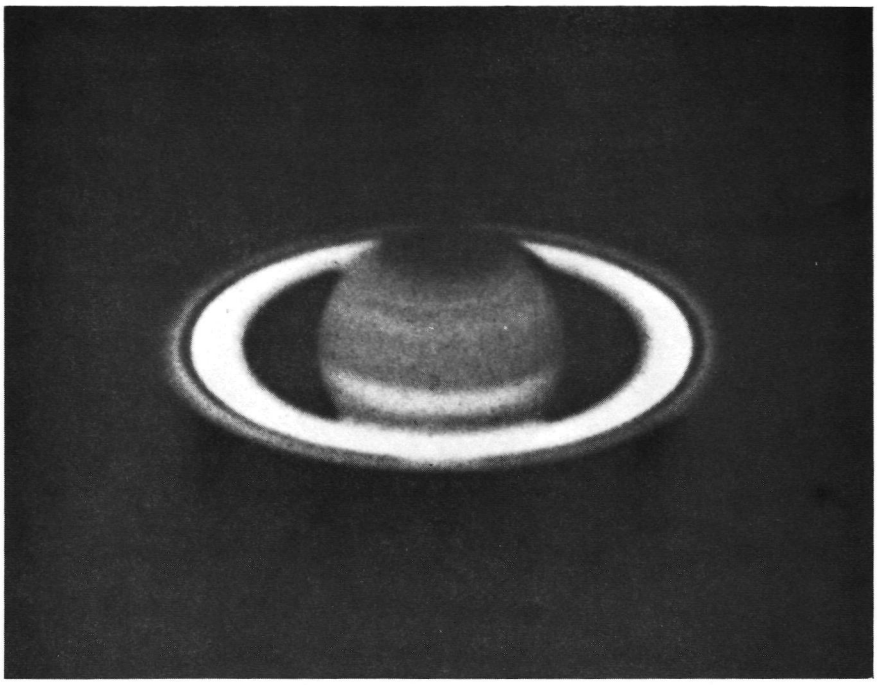

a. Simulated Saturn Image Taken from Kuiper's "Planets and Satellites."

b. Same as above but Taken through the Imaging Spectrometer Optics.

Figure 2-3

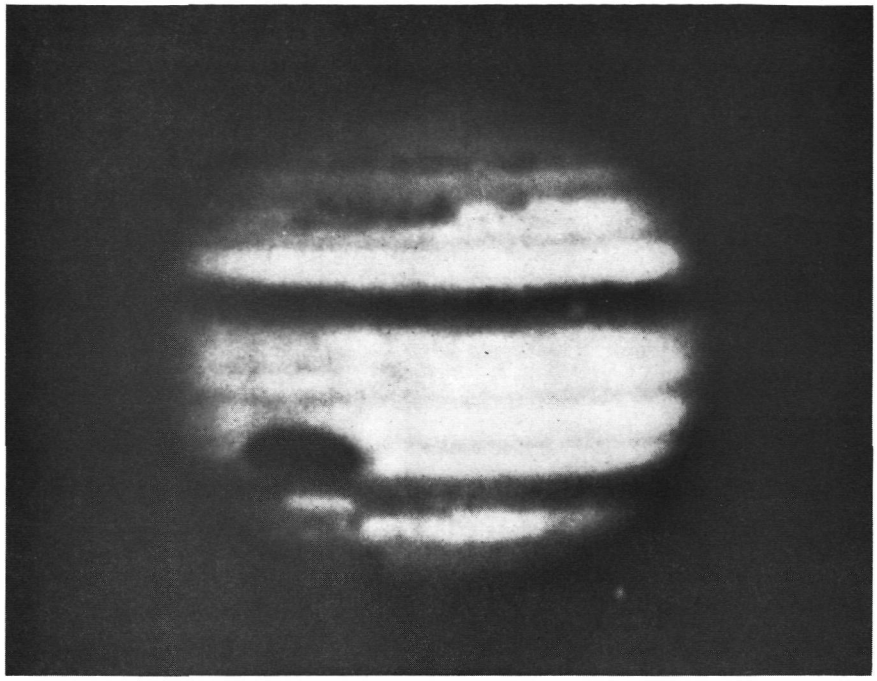

a. Simulated Jupiter Image Taken from Kuiper's "Planets and Satellites."

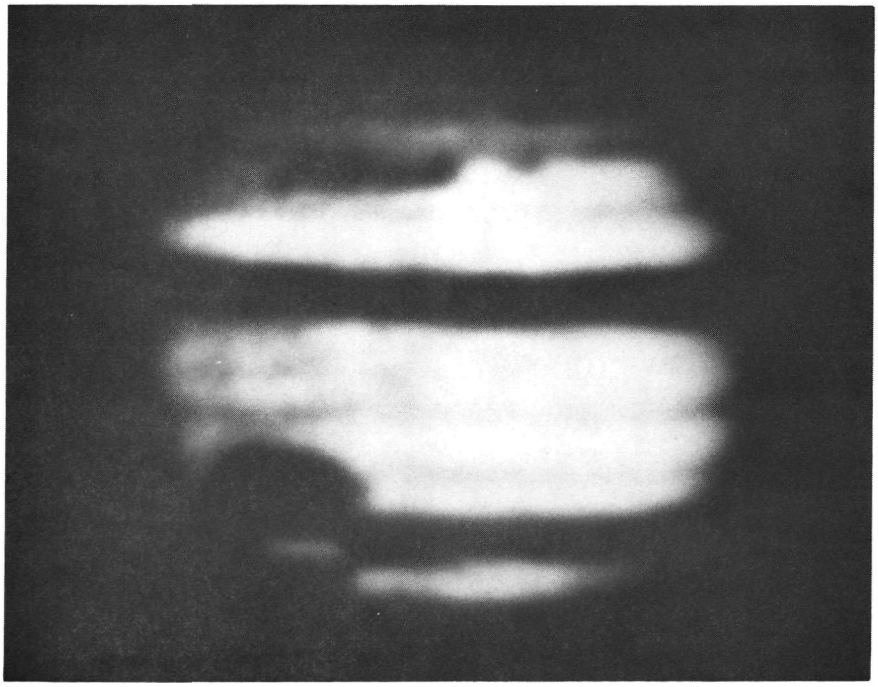

b. Same as above but Taken through the Imaging Spectrometer Optics.

Figure 2-4

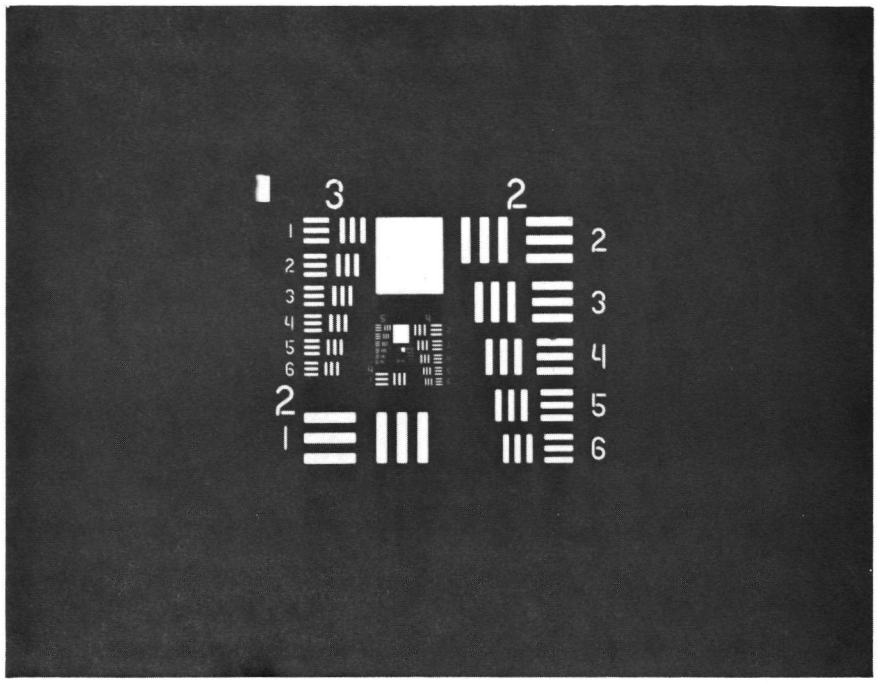

a. Standard Bar Test Pattern. The Bars in Column 3, Row 3 correspond to 0.6 Arc Seconds.

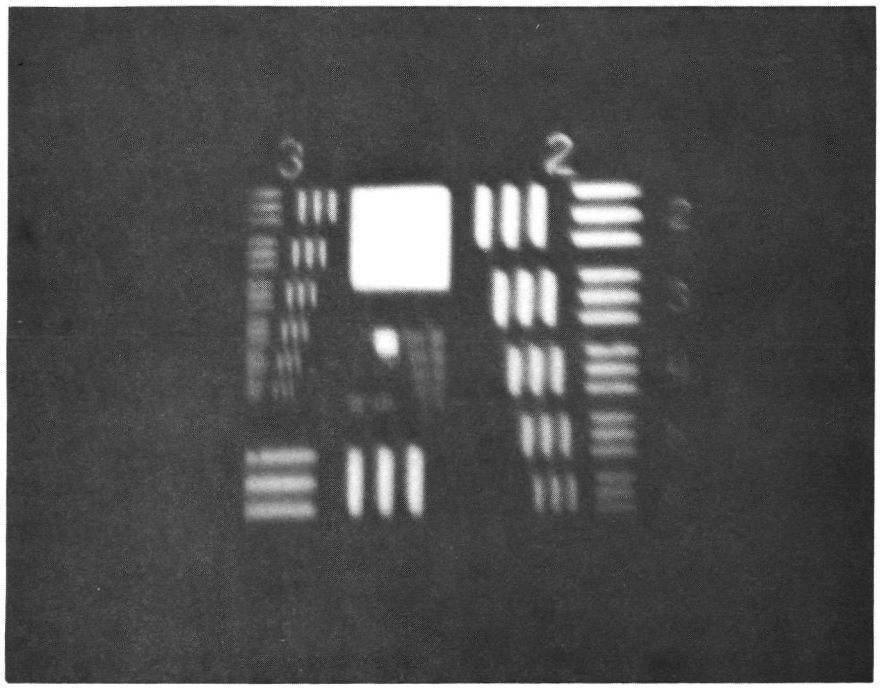

b. Same as above but Taken through the Imaging Spectrometer Optics.

Figure 2-5

TABLE I
Resolution as a Function of Position in the Field of View

Field of View Section	Vertical Resolution (arc seconds)	Horizontal Resolution (arc seconds)
center	0.5	0.5
top	0.7	0.7
bottom	0.7	0.5
left side	0.7	0.6
right side	0.9	0.6

line pairs/arc sec on the sky that can be achieved by the optics. It should be noted that these figures are taken with the ATOFs polarizers in the uncrossed position. Thus, while the optics are identical to the crossed polarizer/ATOF mode (with the exception of the slight re-focusing due to the bi-refringence of the analyzer), this mode cannot be represented without obtaining near IR difference pictures (see section 3.0).

The transmission of the filter and combined optics is shown in Table II. The measurements were done with a United Detector Technology Model 80X photometer and a helium-Neon laser. A comparison of the calculated versus measured values, shown in the table, indicates that the measured values are reasonable if the ATOF's optics were not anti-reflection coated. We believe that an ATOF could now be built which would have close to 80% transmission. See Fig. 2 for the location of the optics.

In addition to the optics discussed above, a thin membrane pellicle, used for a beamsplitter, and an eyepiece and reticle have been incorporated (Fig. 1) into the system. These provide for visual tracking adjustments while exposures are taking place.

2.2 Electrical

A charge coupled device (CCD) TV camera was chosen for our near IR sensor, instead of the charge injection device (CID) camera with preamp modification originally proposed. It was determined that the new Fairchild sensor (the CCD-202) had a quantum efficiency that was comparable to the original CID sensor even though the Fairchild device has only 50% active area. However, the CCD type read-out has a distinct advantage for our application - lower inherent preamp noise. This is due to the fact that only one sensor output at a time is read, unlike the CID where a complete column of sensors must be addressed

TABLE II
Calculated and Measured Transmissions
of the Optical System

Optics	Measured Transmission	Calculated Transmission
1st relay lens and ATOF	0.06	0.075
2nd relay and cylindrical lenses	0.76	0.85
camera window	0.84	0.85
total optics path	0.04	0.05

for injection in order to read a particular sensor's output. Thus the readout capacitance is lower for the CCD than for the CID and hence less read-out noise occurs (the readout noise in RMS electrons is $400 \times\sqrt{C}$ where C is the readout capacitance in picofarads). We estimated an order of magnitude improvement; actually a decrease in the readout noise by a factor of 8 has been observed.

The laboratory experiment used to measure the improvement in sensitivity resulting from the use of the CCD camera was performed as follows. Five interference filters covering the range 7500 Å to 10,000 Å were used along with an apertured, point incandescent source and a relay lens. A small monochromatic disk of light impinged on part of the CCD (or CID) sensor area. For each of the filters the output voltage from the particular camera under test was measured. It was important to keep within the cameras' linear range. Without changing the test set-up in any way and therefore the luminance, the other camera was substituted and its output voltage measured. For each camera an estimate of the RMS fluctuations of an individual sensor was determined by observing many camera output frames on an oscilloscope trace.

Figure 6 shows the results. "R" is the ratio of the CCD camera sensitivity to the CID camera sensitivity at a particular wavelength. Camera sensitivity was determined by taking the ratio of the camera output voltage from the monochromatic disk source of light to the RMS individual sensor fluctuation voltage. Thus while these are only relative measurements, the ratio "R" gives an absolute measure of the cameras' comparative sensitivities. In calculating "R", it was necessary to consider the ratio of the two cameras ' total sensor area and the ratio of the cameras'

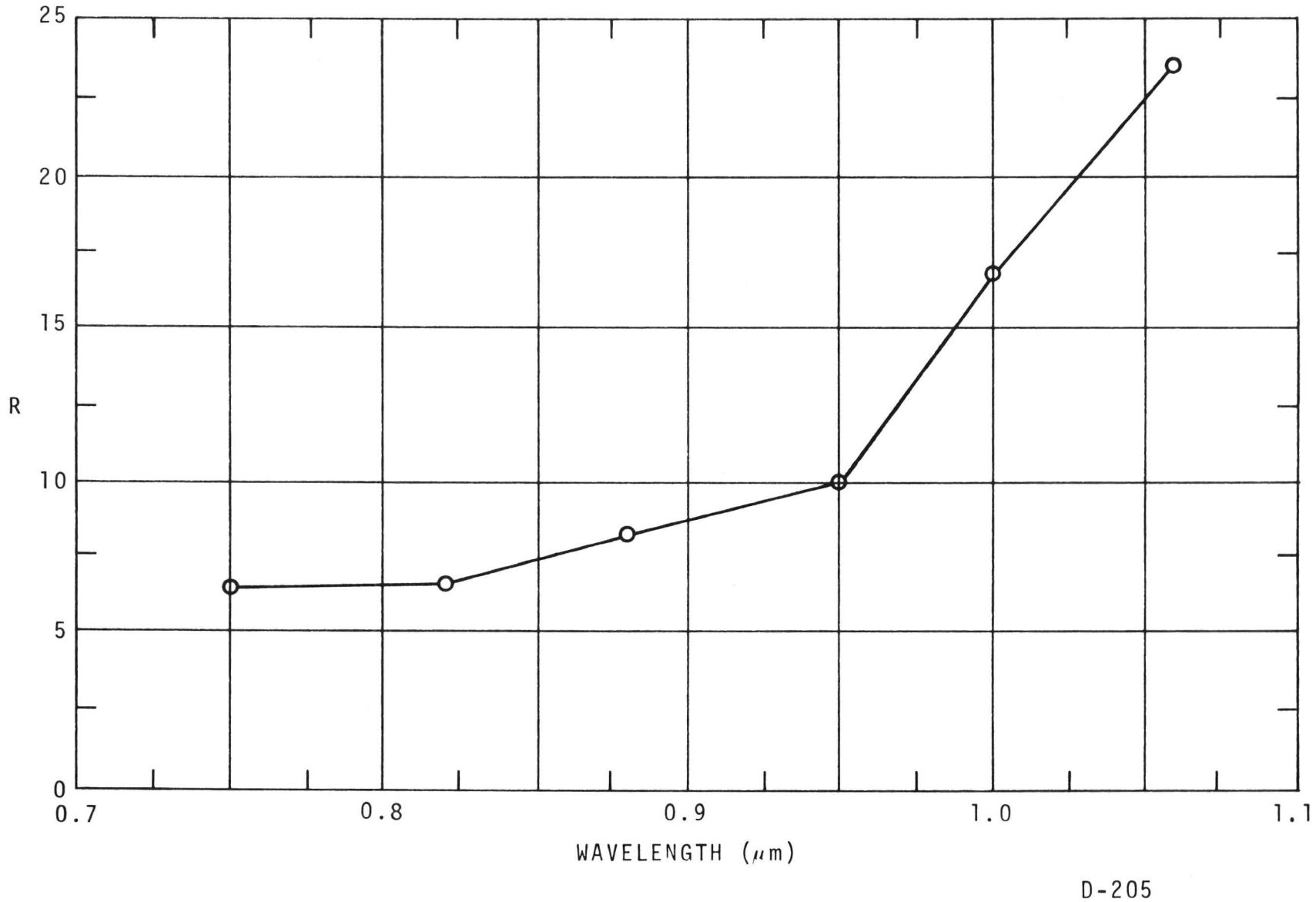

Figure 2-6. CCD Versus CID Sensitivity Ratio.

exposure times. The results indicate that the Fairchild CCD camera is approximately a factor of 8 more sensitive than the G.E. CID camera. As mentioned before this result was expected. We are changing the effective telescope plate scale from 0.9 to 0.6 arc second per pixel, thus a factor of two will be lost in surface brightness on the CCD camera. The exposure times for the upgraded instrument are therefore expected to be about 4 times shorter than for the original instrument.

The computer interface for the new CCD camera was built as part of an AS&E soft X-ray CCD proposal program, although it can be fully utilized for planetary measurements. A block diagram of the CCD camera/computer interface electronics is shown in Fig. 7. Faster sample-and-hold and analog-digital conversion circuits have been employed for the CCD frame time of 200 ms; 12 bit accuracy has been maintained and digital opto-isolators have been used because of the grounding problems experienced at Harvard Observatory. A boxed 19" rack size structure supports all of the CCD/computer interface electronics including all power supplies for the electronics and CCD.

The CCD sensor is cooled to allow for all integration times exceeding a fraction of a second in duration. An alcohol/dry ice slurry and an alcohol transport medium were used previously for the CID sensor cooling. Although this system performed satisfactorily, the need for constant renewal of dry ice and the observation of temperature-dependent dark current variations indicated the need for a more stable, reliable and simpler cooling system. A thermo-electric (T/E) cooling system has been adopted that utilizes a cooler specifically designed for the Fairchild CCD sensor by Cambion, Inc. A T/E module, obtained from Cambion, and a standard regulated power supply have been

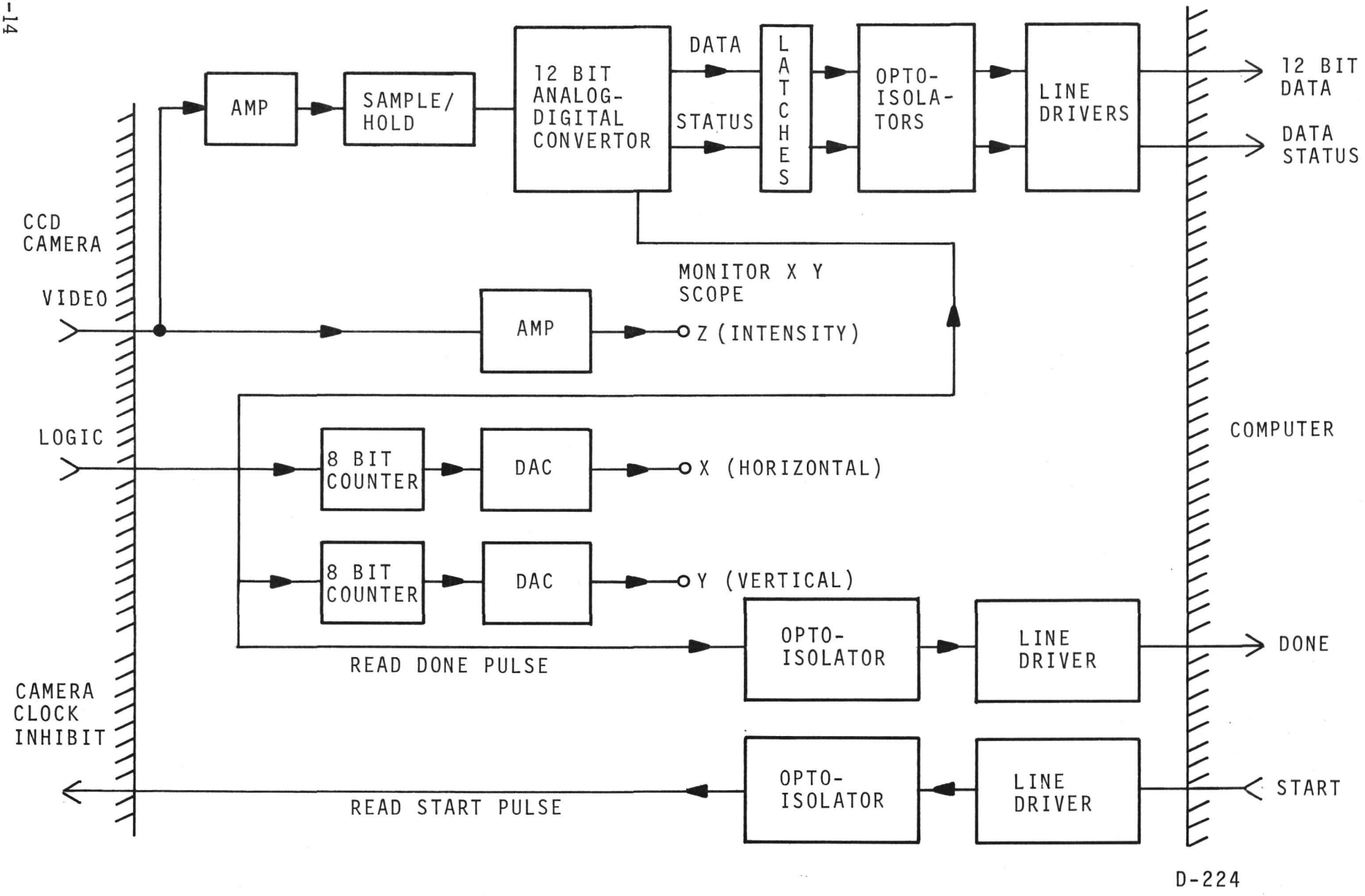

Figure 2-7 CCD/Computer Interface Block Diagram

used. The CCD sensor and T/E cooler have been mounted in an aluminum cylinder and are protected from heat and humidity by styrofoam insulation and an evacuated glass window.

2.3 Mechanical

An optical bench (10" x 36" x 2") was selected from Newport Research Corporation to provide a sturdy, inflexible flat base for mounting the optical components of the imaging spectrometer. The bench is made of two 1/4" aluminum plates supported by an internal honeycomb structure. A 1" matrix of 1/4-20 tapped holes is provided for mounting purposes.

A housing structure that attaches the optical bench to a telescope bolt circle and also supports a light-tight cover has been built (Fig. 1). We have ensured that the plane of the telescope bolt circle is perpendicular (to within several arc minutes) to the optical table base. The optical table support was designed so that it would not flex when the instrument traveled with the telescope in right ascension.

The individual optical components are generally mounted on "I" beams, but with a "V" block mounting for the ATOF, and an optical axis translation stage for the CCD camera mount. The bases of the mechanical mounts are attached to the optical table base by "fingers". These "fingers" allow for great flexibility of positioning and rather fine adjusting of optical components yet they also provide a sturdy support to maintain the relatively close optical tolerances required for the accurate correction of the ATOF air gap. The result of this design is a flexible mounting system for the optical components yet a system where optical integrity can be maintained while the instrument is on the telescope. Changes to the optical set-up can also be made with relative ease in the event that a different component configuration is required.

2.4 Adjustments

The adjustments required to optimize the imaging spectrometer's performance fall into three categories: the ATOF correction optics, the CCD clock voltages and the analog-digital converter (ADC). The rest of the instrument is fully determined except for computer programming (generally accomplished by the Fortran V language inherent in the computer's operating system). The digital format of the data thus allows data correction procedures and display by precisely determined programmed parameters. Of course, brightness and contrast, as well as a complete set of convergence adjustments are available on the color TV computer data display monitor.

The optical train components are removable from the optical Table of the instrument by loosening the attachment "fingers", however, "L" shaped flat pieces of metal held on by "fingers" or washers allow the optical components to be placed back on the instrument in the same precise location as they were before they were removed. Thus, the first relay lens, the ATOF axis alignment, the second relay lens, and the cylindrical correcting lens positions are completely fixed. The best rotation of the ATOF with respect to its V-block holder is indicated by scribe marks. The ATOF can be translated along the optical axis to optimize vignetting for different de-magnification ratios of the system. The ATOFs position along the optical axis does not directly effect the de-magnification or resolution imaging characteristics of the system since the ATOF consists of only flat optical surfaces. The nominal position of the ATOF along the optical axis is such that the 6mm diameter entrance aperture of the ATOF housing is at the exit pupil of the system (the focal length distance of the first relay lens, approximately 4" from the center of that lens).

The CCD sensor array is fixed in height, optimized for vignetting. The critical vignetting (and aberration) adjustment of the CCD's field of view is in the horizontal plane, the plane of the ATOF air gap angle (see Fig. 2). "Fingers" allow for easy adjustment of the CCD camera in the horizontal plane. Focus of the system is done by translating the CCD camera along the optic axis; a micrometer and translation stage are provided for this. Focusing of the system and horizontal positioning of the CCD are best done by observing a source at the optical object plane of the instrument with the XY oscilloscope monitor and the CCD camera in the "free-run" mode. Real-time instantaneous feedback is then available to the experimenter. The horizontal position of the CCD is determined by centering the image in the CCD array when the object is positioned for optimum balanced vignetting.

The instrument's optical object plane was nominally set at 12" in front of the first surface apex of the first relay lens. This provides for a de-magnification ratio of 3:1 when the CCD camera is in focus. Thus a 30μm x 40μm pixel center-to-center spacing on the CCD corresponds to 0.6 x 0.8 arc seconds on the sky for the Harvard 61" reflector (1200" focal length). The ATOF accepts an f/20 beam (Harvard 61" Cassegrain focus f number) producing f/7 at the CCD position. For the Mauna Kea telescopes, the ATOF will accept an f/15 beam with a 2:1 de-magnification (f/7 at the CCD). The 88" telescope has an f/10 cassegrain focus, thus a 60" aperture will be accepted by the instrument, with a CCD pixel projection of 0.5 x 0.7 arc seconds on the sky (880" focal length). The 24" telescope has an f/15 Cassegrain focus, thus the instrument should accept the full aperture but at a reduced plate scale of 1.3 x 1.8 arc seconds per pixel(360" focal length). To adjust the de-magnification of the optics, the CCD is simply re-focussed for a new object plane distance of 10" from the first relay lens surface. Data

indicate that no apparent resolution loss or vignetting is encountered in changing the object distance as described. The 24" Mauna Kea telescope may require even a smaller de-magnification ratio (with attendent light loss) to achieve a more reasonable plate scale, however.

The adjustments of the CCD clock voltages are difficult to describe here as only certain effects of the adjustment are independent of the individual CCD chip. For the case of the Fairchild CCD-202 sensor array presently used on the instrument, only the clock "high" voltages need be adjusted; the "low" camera clock potentiometers are all set at zero as per the CCD-202 specification. The general effects of varying these four clock "high" voltages are: Horizontal CCD shift register clock - horizontal smearing, image shading and loss of image if too far out of adjustment; vertical CCD shift register clock - similar to horizontal except vertical smearing; photogate clock - too low a setting produces low saturation threshold, too high a setting produces inefficient transfer to vertical registers; reset clock - changes overall image brightness; electronic noise appears in image and seems to be minimized by this setting. The camera also has a gain adjustment and a sample/hold adjustment potentiometer. We have not changed these last two camera settings.

The ADC digitized system has course gain and offset and fine gain and offset controls. The fine controls are usually set to nominal center positions unless very accurate voltage - digital correspondence is required. The course gain is generally set at maximum (then a 1 V p-p video signal from the CCD camera produces a 4 V p-p video voltage for the ADC corresponding to approximately half scale). The course offset is adjusted so that the minimum video (dark with "free-fun" mode) sits at -3 volts into the ADC (or sample/hold amplifier). This will correspond to ~ 1000 digital units on the computer.

3.0 TESTS AT THE HARVARD 61" REFLECTOR

The imaging spectrometer's operation has been tested at the Harvard 61" telescope. The combined data from the tests show the improved spatial resolution of the upgraded instrument and a sensitivity that will allow constraints to be placed upon present atmospheric models of Jupiter. The increase in spatial resolution is indicated primarily by a simulation performed on-site at the 61" telescope. Sensitivity has been determined by a few spectral images taken of Saturn. Venus observations, displayed as 16 spectral images, show contoured isophote shape change as a function of intensity. The Venus data indicate the presence of quantitative photometric data in the images. Unfortunately, the "seeing" conditions at the site during our observing run prevented reasonable spectral image observations of Saturn. A log of the observations and simulations performed at the 61" reflector is shown in Table III.

The instrument has been tested with a simulated image of Saturn, but with the remainder of the experimental set-up identical to that used in recording real images. The instrument was placed on the Cassegrain platform of the 61" telescope with the simulated image of Saturn at the correct distance from the first relay lens. The simulated image is a 35mm slide taken from Kuiper's Planets and Satellites, and the scale of the slide image has been chosen to match the plate scale of the 61" telescope. (We note that the visual filter used to make the 35mm slide yields a different ratio of ball-to-ring intensity than is actually recorded with the imaging spectrometer in the near infrared) The intensity of the light source behind the slide was adjusted so that approximately the same brightness was recorded as we had obtained by observing Saturn through the 61" reflector.

TABLE III

OBSERVING LOG

DATE	OBSERVATIONS (if any)	"SEEING"*
4/6		cloudy
4/7		cloudy
4/8	Saturn, Arcturus	fair
4/9	Sirius , Jupiter, Saturn	good
4/10	Jupiter, Saturn	fair
4/25	CCD adjustments	cloudy
4/28	Sensitivity tests	cloudy
4/30	Saturn	fair-then very poor
5/1	Saturn	poor
5/4	Saturn slide simulation	cloudy
5/5		cloudy
5/6		cloudy
5/7	Saturn - 35mm pictures	poor
5/8		cloudy
5/9		cloudy
5/10	Saturn slide simulation	cloudy
5/14	Venus (morning)	fair

* "Seeing" conditions - estimate of star image blurring: good, ~ 3 arc seconds, fair, ~ 5 arc seconds, poor >7 arc seconds.

The simulated images of Saturn were recorded as if the instrument were on the telescope. The RF signal to the ATOF and the frame initiate commands from the computer were transmitted over 100 foot cables from the computer room. Digital data were also returned to the computer via 100 foot cables. The CCD chip was cooled and 120 second integrations were made (the exposure time needed to obtain a reasonable signal-to-noise with Saturn on the 61" reflector). Images were recorded with and without power to the ATOF. The latter images allow the leakage continuum image, thermal noise from the on-chip preamplifier, and defective picture elements to be subtracted from the spectral image.

The results are shown in Figure 8. The two exposures plus the difference frame are shown. The dark band between the lower ring and ball indicates a spatial resolution of at least ~ 2 arc seconds was achieved by the simulation.

The actual observations made with the imaging spectrometer on the telescope included Venus and Saturn. The Venus observations were made with the full working system and will be discussed later. Our attempts to observe Saturn with the instrument fully operational were unsuccessful. On April 9, 1977, Saturn was observed with the ATOF's polarizers crossed and power applied to the ATOF, but RF interference rendered the images useful only for a sensitivity test. The data did indicate, however, that a signal-to-noise ratio of ~ 30 could be achieved with a 120 second exposure at the 61" reflector. After the RF interference was eliminated, no suitable observing nights for Saturn occurred.

Several images of Saturn were taken with the ATOFs polarizers uncrossed but with a 100 Å interference filter placed in the light path. For these pictures a 30-second exposure was used. One of these Saturn images is compared to a similar image taken on

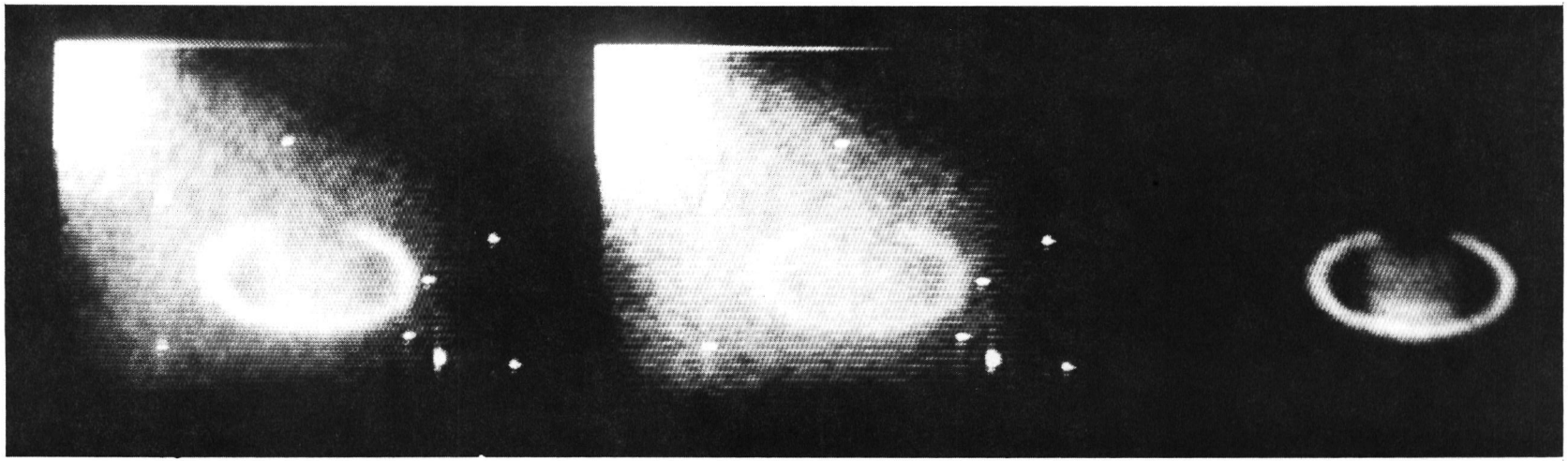

CY - 165

Figure 3-1 Simulated Image of Saturn taken through the completed instrument at Harvard's 61" reflector. From left to right: Origional Image, RF power on; "Leakage" Image, RF power off; Subtracted, monochromatic image (8500 Å). Note brightess distribution emanating from upper left hand corner due to on-chip preamp heat during the two minute exposures. Bright spots are blemishes or bad pixels on the CCD chip.

35mm film (on a different night) in Figure 9 . Both are 30 second exposures, one through the optics of the imaging spectrometer and via the CCD and computer display, and the other recorded directly on film at the f/20 Cassegrain focus of the 61" reflector. The "seeing" was somewhat poorer on the night that the 35mm picture was taken (~ 7 arc seconds) than on the night the CCD image was recorded (~ 5 arc seconds).

The observations of Venus were made on the morning of 14 May, 1977 from approximately 6-11 A.M., EDT. The sky was quite clear but the "seeing" still included some small amplitude scattering of at least 5 arc seconds. We recorded 160 spectral images included 20 of the sky and 140 of Venus. Almost all of the Venus images were 3 second exposures, taken with the ATOF's polarizers crossed. About 2/3 of the images were taken with power applied to the ATOF; the remaining 1/3 were reference images for subtraction purposes. The RF frequencies applied to the ATOF ranged from 18.89 MHz to 32.97 MHz (11000Å to 7500Å).

Two sets of spectral images of Venus are displayed here. One set encompasses a major part of the wavelength range of the instrument taken at 250Å intervals (Fig. 10)and the other set encompasses the CO_2 $5\nu_3$ bandhead region at 8700Å taken at 7Å intervals (Fig. 11). All of the Venus images have been displayed with the same parameters. The images have been corrected for instrumental vignetting by dividing them, on a pixel by pixel basis, by a monochromatic sky image taken at 8500Å. The different size of the images is due to variations of "seeing" and to the reference frame subtraction process. The latter effect is eliminated with somewhat better telescope tracking.

The quality of the images in Figs. 10 and 11 is actually somewhat superior to the qualitative impression formed while viewing Venus

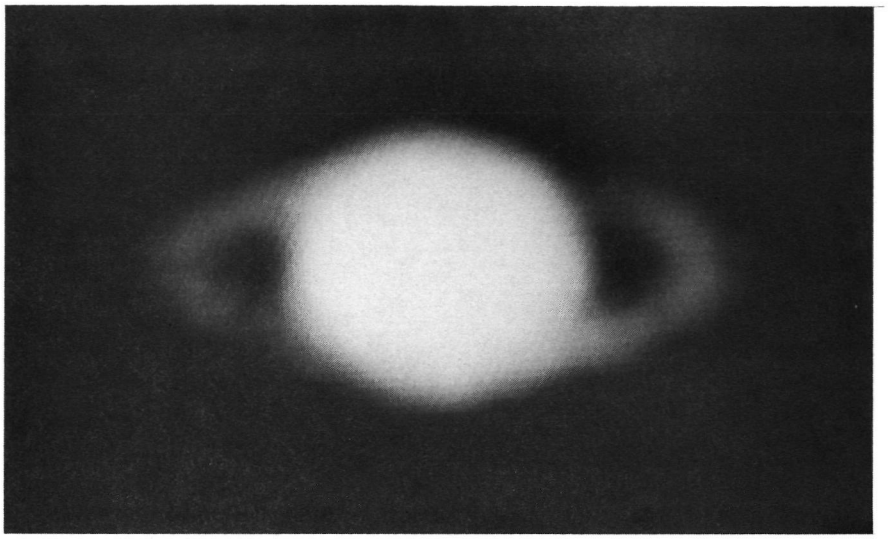

A.

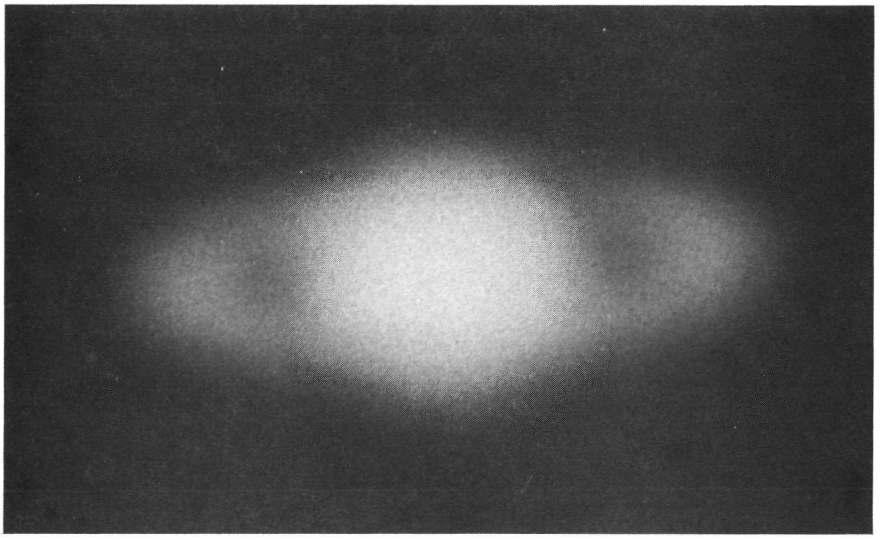

B.

Figure 3-2 Comparison of Saturn Images. A) CCD Image through the instrument with a 7500Å interference filter and a 30 second exposure. B) 35 mm film image taken directly at the f/20 Cassegrain focus of the 61" reflector.

Figure 3-3

(Following Page)

Eight monochromatic (~ 15Å pass band) images of Venus. Numbers below images are wavelengths in Å. All images are displayed with the same parameters and are pixel by pixel ratios of monochromatic difference data to correct for instrument vignetting. Wavelengths cover most of instrumental range.

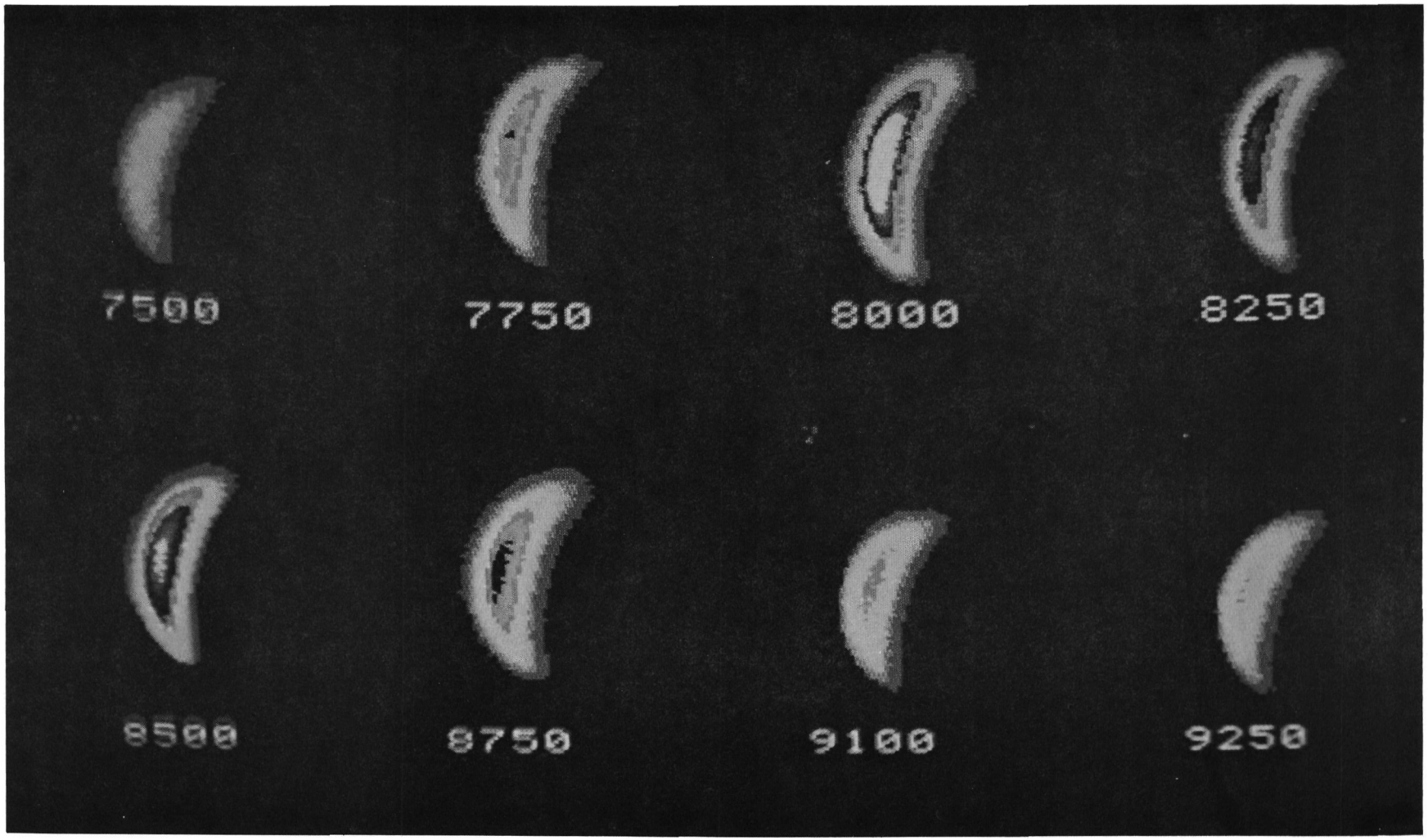

CY-167c

Figure 3-3

Figure 3-4

(Following Page)

Eight monochromatic (~15 Å pass band) images of Venus. Numbers below images are wavelengths in Å. All images are displayed with the same parameters and are pixel by pixel ratios of monochromatic difference data to correct for instrument vignetting. Wavelengths cover region centered on CO_2 $5\nu_3$ bandhead.

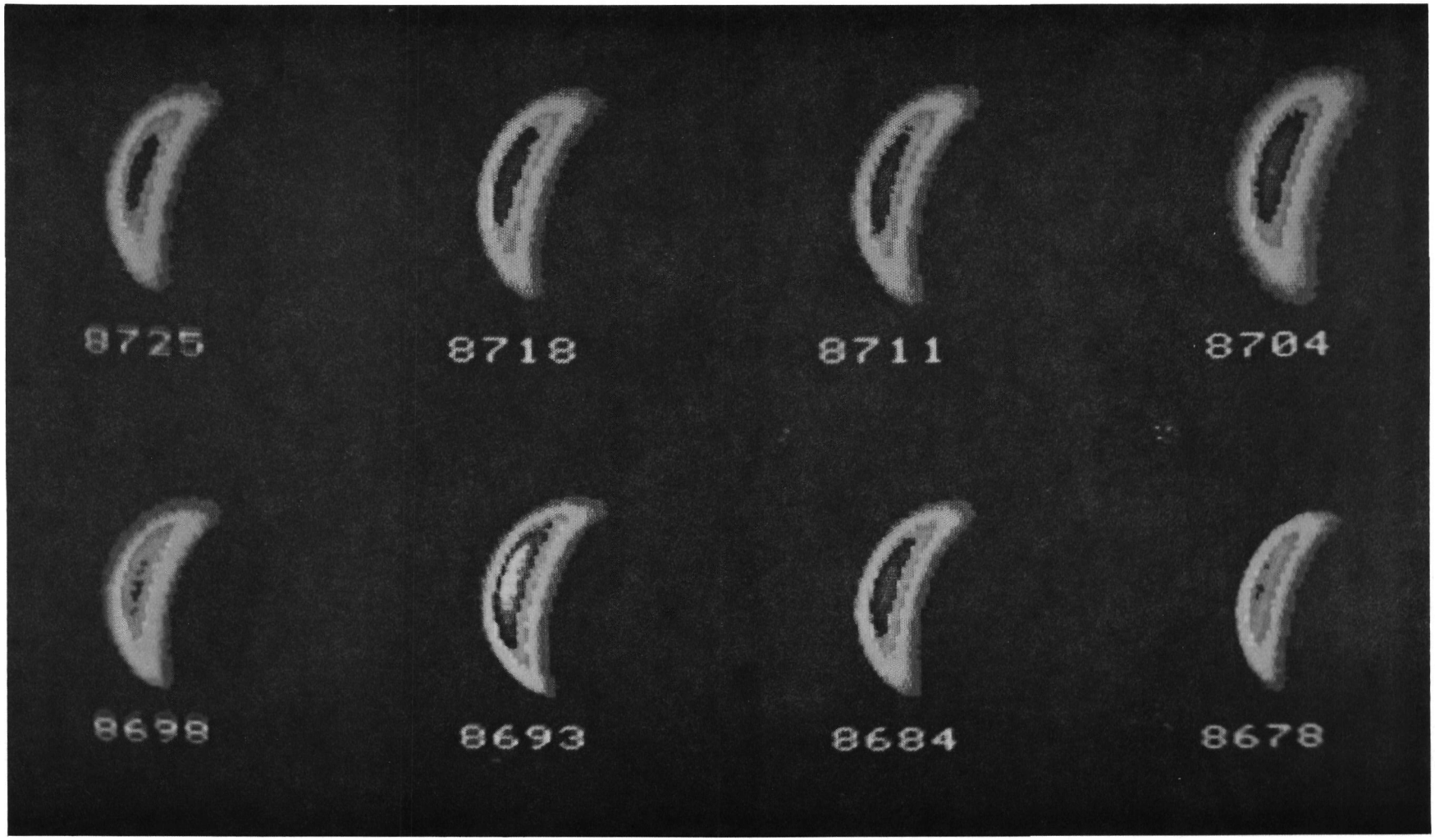

CY-168c

Figure 3-4

through the telescope. In Fig. 10 the shape of the crescent remains about the same but the overall intensity of the images changes over the wavelength range of the instrument. This is due to the reduction of the ATOF efficiency on the short wavelength end of the spectrum and of the transparancy of the silicon CCD sensor on the long wavelength end. The spectral images taken across the CO_2 band are similar to each other in appearance. There does not seem to be a significant intensity dip as the CO_2 $5\nu_3$ bandhead is scanned. This is likely due to the relatively large passband (~ 15Å) of the instrument, compared to the ~ 1Å equivalent width of the bandhead. Quantitative limb darkening studies of these images may reveal some subtle difference within the bandhead region.

4.0 SUMMARY AND CONCLUSION

The basic goals of the upgrading program for the ATOF/CCD imaging spectrometer have been accomplished (Appendix A describes the original instrument). The instrument's spatial resolution and sensitivity have been improved to the point that meaningful observations of Jupiter can be done at a good site. In particular, we have refurbished the instrument optically, electronically and mechanically and have demonstrated its performance at Harvard's 61" reflector.

The optical refurbishment consisted of designing correcting optics for the ATOF. The ATOF has an integral air gap that results in astigmatism and coma aberrations. Computer ray tracing has been performed and achromatic lenses built to our specifications. Laboratory tests have shown better than 1 arc second projected sky resolution for the instrument.

The electrical refurbishment has consisted of replacing the camera previously used in the instrument with a more sensitive CCD camera. The computer interface electronics have been re-designed for the new camera. Opto-isolaters have been used in the data transmission lines to ensure stable performance in the field. Cooling of the camera sensor has now been provided by a thermo-electric system. The present instrument has a measured sensitivity approximately 4 times better than the previous one (with a plate scale of 0.6 arc seconds per pixel as compared to 0.9 arc seconds per pixel before).

The mechanical refurbishment of the instrument has allowed for a much more flexible system of component mounting. The components are mounted to a sturdy optical table which is held onto the telescope by a rigid housing and circular flange.

The upgraded imaging spectrometer was tested successfully at Harvard's 61" reflector during April and May 1977. The sensitivity improvement was checked by observing Saturn (although site "seeing" did not allow good observation). Simulations performed on site show the spatial quality of image data that can be obtained from the instrument. Observations of Venus, recorded May 14, 1977 indicate the type of photometric data obtainable. Representative image data have been included in this report.

In conclusion, we believe the tests at the 61" telescope indicate that the imaging spectrometer has sufficiently good spatial resolution and sensitivity to perform meaningful observations at a good site. The simulated images show sufficient spatial resolution to identify local band features on both Jupiter and Saturn. The observations of Venus indicate the potential for quantitative interpretation of monochromatic image data.

We are proposing to study the verticle structure of the upper Jovian atmosphere with the instrument at Mauna Kea Observatory. Detailed analysis of the spectral image data would be performed using existing radiative transfer techniques. Atmospheric model parameters are now under-constrained. Photometrically calibrated, monochromatic planetary images can provide many of the necessary constraints. The advantage of this technique over previous ones utilized for planetary measurements include: simultaneous recording of the entire disk of the planet, narrow pass band (~ 15Å) and spectral sensitivity out to nearly 1.1 micron. This latter feature allows measurement of the strong methane and ammonia bands located at 0.725, 0.89 and 1.05 microns. The data included in this report indicate the need to utilize the instrument at a site where better "seeing" conditions prevail. Then the technique of imaging spectroscopy represented by the ATOF/CCD device discussed here will be able to prove itself in planetary research.

APPENDIX A

ASE-3685

PLANETARY INVESTIGATION UTILIZING AN IMAGING SPECTROMETER SYSTEM BASED UPON CHARGE INJECTION TECHNOLOGY

R. Wattson, P. Harvey and R. Swift

American Science and Engineering, Inc.
Cambridge, Massachusetts 02139

Submitted to and Accepted by:

The Symposium on Charge-Coupled Device Technology
for Scientific Imaging Applications

Jet Propulsion Laboratory
Pasadena, California

6-7 March 1975

ABSTRACT

An intrinsic silicon charge injection device (CID) television sensor array has been used in conjunction with a $CaMoO_4$ co-linear tunable acousto-optic filter, Harvard's 61-inch reflector, a sophisticated computer system, and digital color TV scan converter/computer to produce near IR images of Saturn and Jupiter with 10Å spectral resolution and ~ 3" spatial resolution.

The CID camera has successfully obtained digitized 100 x 100 array images with 5 minutes of exposure time, slow-scanned readout to a computer (300 ms and digitized to 12 bits accuracy) and has produced this data at near dry ice temperature and in conjunction with other state-of-the-art technology instrumentation. Details of the equipment setup, innovations, problems, experience, data and final equipment performance limits are given, so that those people who plan to utilize solid-state TV sensor arrays will be able to judge, at least in part, which technology, CCD or CID, they should choose. Twelve spectral images of Saturn are shown, 40Å apart (centered at 8500Å), which will illustrate the type of data now obtainable with present CID technology. It is our belief that the data represents the first instance of truly three-dimensional astronomical data that has been obtained.

1. Introduction

Figures 1(a) and (b) are images of Saturn having ~ 3" spatial resolution. Each image represents a 10Å spectral bandpass in the near infrared, and required about 5 minutes of exposure due to the narrow bandpass. The twelve spectral images of Figure 1(a) are generally 40Å apart, as indicated by the central wavelengths shown below each image (the first image should indicate 9400Å). Although some corrections for background and noise have been applied, it is not valid to compare the overall intensities of different spectral images. However, the variation of ball to ring intensity ratios for the different images is significant. The absence of Saturn's ball at 8900Å and 8860Å and the depression of the ball relative to the rings near 8700Å is clearly evident. Note also the bright equatorial bulge in the planet seen at 8780Å. This may be caused by higher clouds and hence less methane absorption near Saturn's equatorial region. It is interesting to compare the relative ball to ring intensities vs wavelength with the reflectivity spectrum of Jupiter shown in Figure 2, from Pilcher et al.[1] The dots, indicating the wavelengths of the Saturn images of Figure 1(a), encompass a methane double absorption feature with a strong dip at 8900Å and a more moderate dip at 8700Å. The spectral resolution is 10Å in both Figures 1 and 2.

Figure 1(b) shows both a spectral image of Saturn (8660Å) and a spatial intensity plot for a line through the planet. The location of the line is indicated by tick marks on the image. Note the good S/N (~20:1) of the plot. The intensity scans for Saturn's ball are essentially limb-darkening curves. These curves are being analyzed by fitting to Minnaert functions for various wavelengths.

These and other spectral images of Saturn, ranging from 7200Å to 10,600Å (i.e., essentially the range covered by Figure 2), and a similar set of images of Jupiter, were obtained from data taken at Harvard's 61" reflector during December 1974 and early January 1975. They were acquired by the use of a new type of instrumentation, an imaging spectrometer, which is the subject of this paper.

2. Description of Instrumentation

Figure 3(a) shows a schematic of the Imaging Spectrometer. Figure 3(b) is a picture of the instrument which is about two feet long. It consists of two principal parts: a tunable acousto-optic filter (TOF)[2] and a charge injection device camera (CID).[3] The TOF is similar in throughput and transmission characteristics to an interference filter of comparable resolution, except that it is electronically tunable over a 2:1 wavelength range. The TOF utilizes a pair of crossed calcite Glan-Thompson polarizers, between which is placed a bi-refringent $CaMoO_4$ crystal. Acoustic waves, produced by a voltage-controlled oscillator and piezoelectric transducer, are propagated axially through the bi-refringent crystal and absorbed at the opposite end. Polarized light transmitted through the crystal in a direction co-linear with the acoustic waves interacts with the acoustic field in such a way that only a narrow range of wavelengths, related to the acoustic frequency, is scattered into the other polarization state and is thus transmitted by the output polarizer. The filter's bandpass is basically determined by the same characteristic that determines the bandpass of a diffraction grating monochromator: the number of grating rulings; correspondingly, in the TOF, the number of acoustic waves in the crystal determines its resolution. Computer control of the r.f. driving frequency is possible.

The other optics of the imaging spectrometer include relay lenses to transmit the primary telescope image through the TOF and onto the CID chip; a beam splitter, reticle and eyepiece which are used for manual guidance of the telescope during exposure; and a cylindrical lens to correct for the astigmatism produced by the TOF's bi-refringence.

The CID camera is basically an intrinsic silicon 100 x 100 sensor array, wherein each sensor is ~ 0.1mm square. Each sensor has a quantum efficiency of ~ 50% at 9000Å and, at -40°C, shows only moderate integrated dark current after 5 minutes exposure time. The CID, like the CCD cameras, employs a passive solid-state digital read-out mode instead of either the active digital read-out mode of photodiode arrays such as Reticon arrays or an electron-beam read-out mode as exemplified by the silicon target vidicon cameras. Highly monochromatic radiation, such as is used in this system, may produce interference effects in a vidicon system. No such effect has been observed with the present TOF/CID system having a 10Å bandpass.

The charge injection device read-out employs the injection of a particular sensor's charge into the silicon substrate via the voltage change across a row/column addressed capacitor at the sensor site. Other sensor sites along the particular row or column only have their charges shifted. With this technique random sensor interrogation could be achieved if desired. Charge coupled technology, on the other hand, requires many transfers via capacitor plates to translate the entire charge pattern resulting from the image to a storage area for line by line read-out, thereby requiring extremely high transfer efficiency.

The GE CID camera, which was originally designed for standard TV frame rates, had a read-out rate fixed at about 300 kHz continuous, and used a triggered analog sweep system, so that after injection significant amounts of signal remained uncollected. At AS&E the camera was modified by installing interrupt circuitry to hold the digital camera sweep at the beginning of the first field until triggered by a computer, one sweep at a time. The injection time was increased and the internal read-out clock rate decreased;

a digital monitor sweep system was constructed which would track the camera sweep regardless of rate. The output signals were amplified, DC restored, digitized, and sent via line drivers to the computer.

The CID chip was found to saturate on dark current in about 3 seconds at room temperature. Since the expected signals would require integration for much longer periods of time, it was necessary to cool the CID chip to reduce both the dark current and its associated shot noise. The characteristics of reverse-biased Si are such that the dark current can be expected to decrease approximately a factor of two for every 10^{o}C cooling. Thus, at the temperature of dry ice, or some 100^{o}C below room temperature, we would expect to be able to integrate for about a half hour without dark current saturation.

In order to achieve such cooling, the CID chip was removed from its socket in the camera body and mounted on an ~ 1 inch extender, so that it could be located within a cooled, insulated enclosure. The extender was fabricated from a spare header and socket, provided by GE, sandwiched around a block of lucite. The interconnections were made by means of fine (#30) wire to minimize heat conduction. The enclosure is (literally) a peanut can, lined with polystyrene foam and provided with a double-paned window, evacuated between the panes to provide a thermal barrier that does not frost. The assembly was attached to the camera body at the normal lens location. The enclosure was continuously purged with dry nitrogen gas to prevent fogging.

Cooling was done by thermally coupling the CID to a brass heat sink, through which cold alcohol was pumped. Anhydrous, denatured alcohol and 1/4" tubing were used to prevent the fluid viscosity from restricting the flow. Several coils of copper tubing

immersed in a dry ice/alcohol slurry served as a heat exchanger through which the coolant was circulated. The slurry temperature was about $-55^{o}C$. This operating temperature for the CID chip is consistent with dark current saturation after $\approx$ 20 minutes. Dark current buildup was hardly detectable after 5 minutes of integration time.

Experience with the CID camera, operated under extremely cold ($-15^{o}C$) and also under humid ambient conditions, showed that modification and refurbishment of both the prototype electronics and the CID sensor array was needed. With strong co-operation from GE, both were done. Because of the longer injection times and the small capacitances involved in the read-out circuitry, the printed circuit board became a significant leakage path due to condensation or humidity in the telescope environment. The problem was overcome by thoroughly cleaning and drying the board and spraying it with Krylon clear plastic. Hermetic sealing of the CID chip, to overcome moisture contamination problems, was done at GE. Very little difficulty with the CID camera has been experienced since these changes were made. The data and accumulated experience indicate that the expertise now exists to allow reliable field use of CID cameras, at least for ground-based observational purposes.

Frame integration time was determined by the operator, who had control of the system via an alphanumeric computer terminal. When the program determines that an exposure is complete, the computer initiates the CID read-out mode. The 10^{4} word, 12 bit read-out of the CID camera was read directly into the 32K core of a NOVA 1200 via the data channel. The data were then stored on digital tape and, for random access to spectral image frames, stored also on magnetic disc.

One of the main design philosophies of the system was real-time display of the data, allowing the operator to exercise his judgment to repeat exposures and/or modify or improve the data acquisition parameters based upon the observed results. Hence a display computer/scan converter and a color TV monitor were used to immediately view the images as they were acquired. The use of color can enhance the observer's ability to discriminate against improper data. Some degree of processing can also be accomplished before display. Various other display modes such as alphanumeric information and plots are available at the operator's command. The images shown in Figure 1 were produced directly via this display system.

Finally, the entire computer support facility (shown in Figure 4) is portable. It is sufficiently small and reliable to be transported and operated anywhere, having already been used at several sites without major difficulty.

3. Conclusions

The data displayed here represents only the first very preliminary and relatively crude data obtained by an imaging spectrometer system designed for astronomical observations. Improvements of factors of 3 or more in instrumental sensitivity, spatial resolution and demonstrable spectral resolution can be made by improved CID preamp design, reduced residual bi-refringent aberrations and extended observation time. Careful photometric calibration and spatial, spectral and vignetting corrections, combined with use of observation sites more suited to planetary observations (i.e., observation sites where relatively long exposures can be accomplished with 1" or better "seeing" and guiding characteristics), will provide very useful new planetary results. Extension of the spectral response to the 5μ region is possible by the use of InSb CID's and TeO_2 TOF's. Observation sites located above the Earth's atmosphere would eliminate atmospheric interference in that spectral region, and would extend the spatial resolution to the diffraction limit. Finally, sophisticated radiative transfer algorithms employing anisotropic, inhomogeneous atmospheric modeling will enable one to construct, via planetary atmospheric molecular absorption features, truly three-dimension pressure, temperature, constituent and aerosol maps of planetary atmospheres. Such pixel by pixel "sounding" maps can be made with the existing equipment for CH_4 and NH_3 on Jupiter and Saturn, CO_2 on Venus and, in fact, the present spectral resolution may even allow 1" maps separating the J-manifolds of the R-branch $3\nu_3$, CH_4 band! Hence one could say that the technique described above represents the beginning of true 3-D planetary astronomy.

Much appreciation is extended to the directors and staff of the Harvard Observatory for their strong cooperation in the observa-

tional program. The authors would also like to thank Dr. Edwin Frederick and Dr. Saul Rappaport as co-observers, and Richard Cabral and Douglas Hill for their very helpful engineering in this effort.

4. References

1. C. B. Pilcher, R. G. Prinn and T. B. McCord; J. Atmos. Sci., 30, 302 (1973).

2. S. E. Harris, S. T. K. Nieh, and D. K. Winslow, "Electronically Tunable Acousto-Optic Filter", Applied Physics Letters, 15, 325 (1969).

3. G. J. Michon and H. K. Burke, "Charge Injection Imaging", IEEE International Solid-State Circuits Conference Digest, 138-139, (1973).

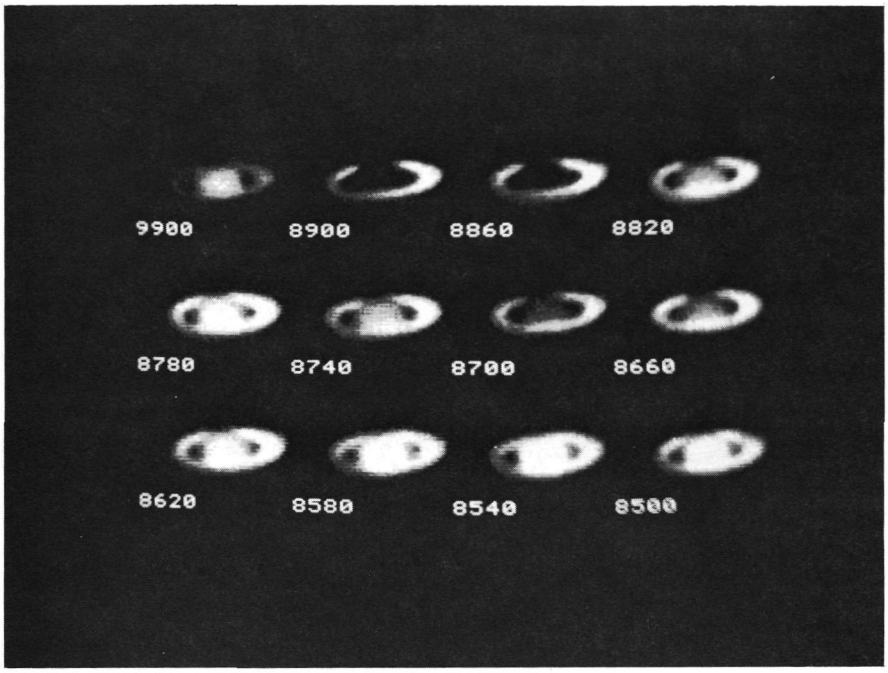

CY-117

Figure 1(a). Twelve Images of Saturn at Wavelength Ranging From 8500Å to 9400Å (See Text)

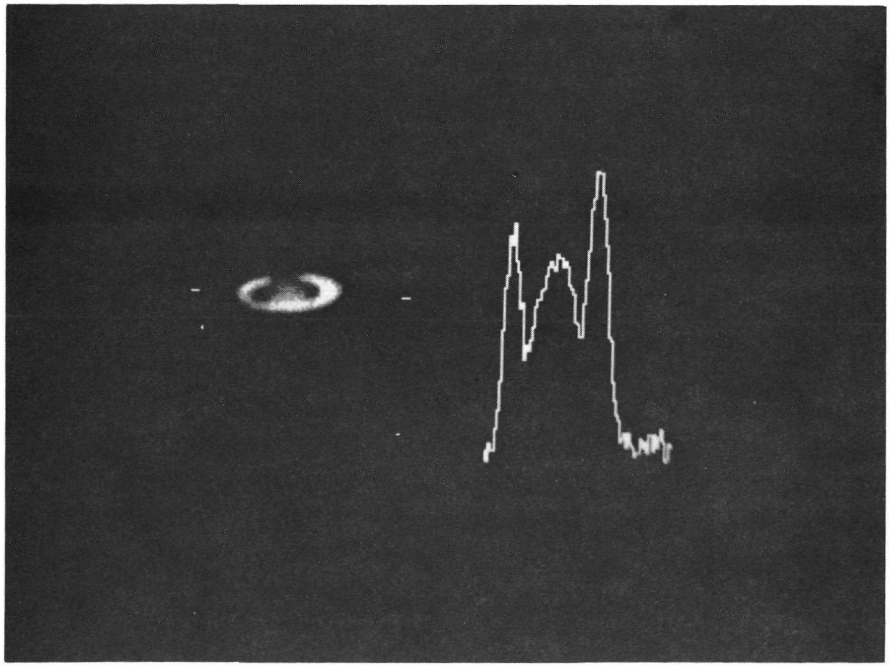

CY-124

Figure 1(b). Spectral Image and Cross Sectional Intensity Plot of Saturn at 8660Å

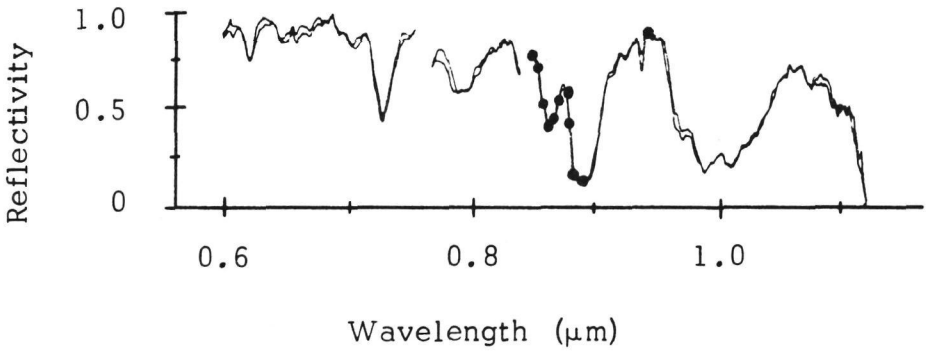

Figure 2. Absolute Reflectivities of Jupiter [1]

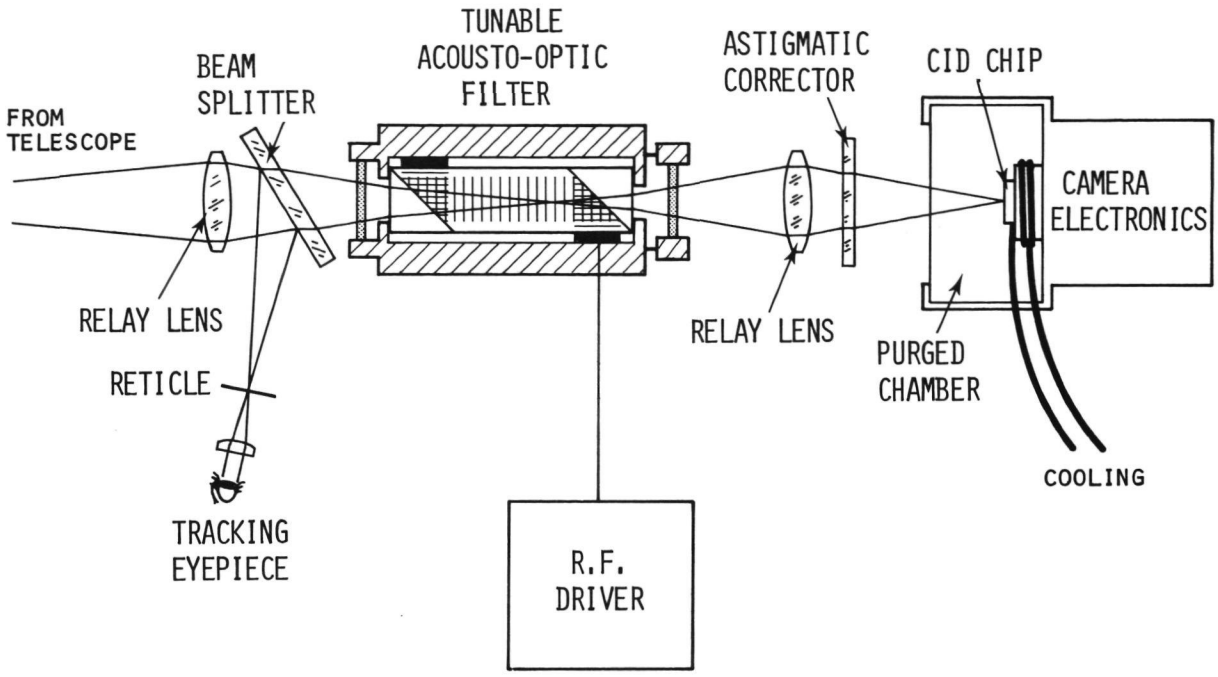

Figure 3(a). Schematic Diagram Showing Principal Components of the Imaging Spectrometer

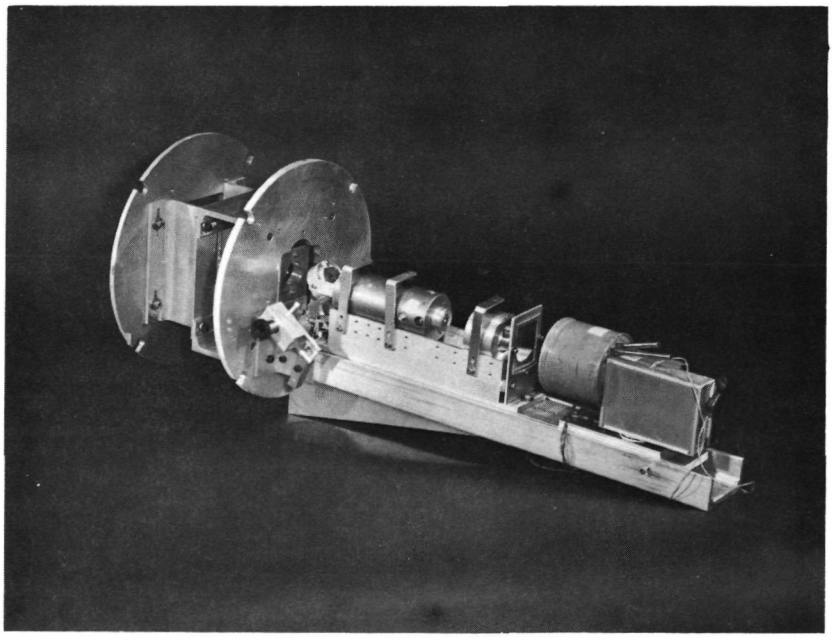

CY-114

Figure 3(b). Photograph of the Imaging Spectrometer

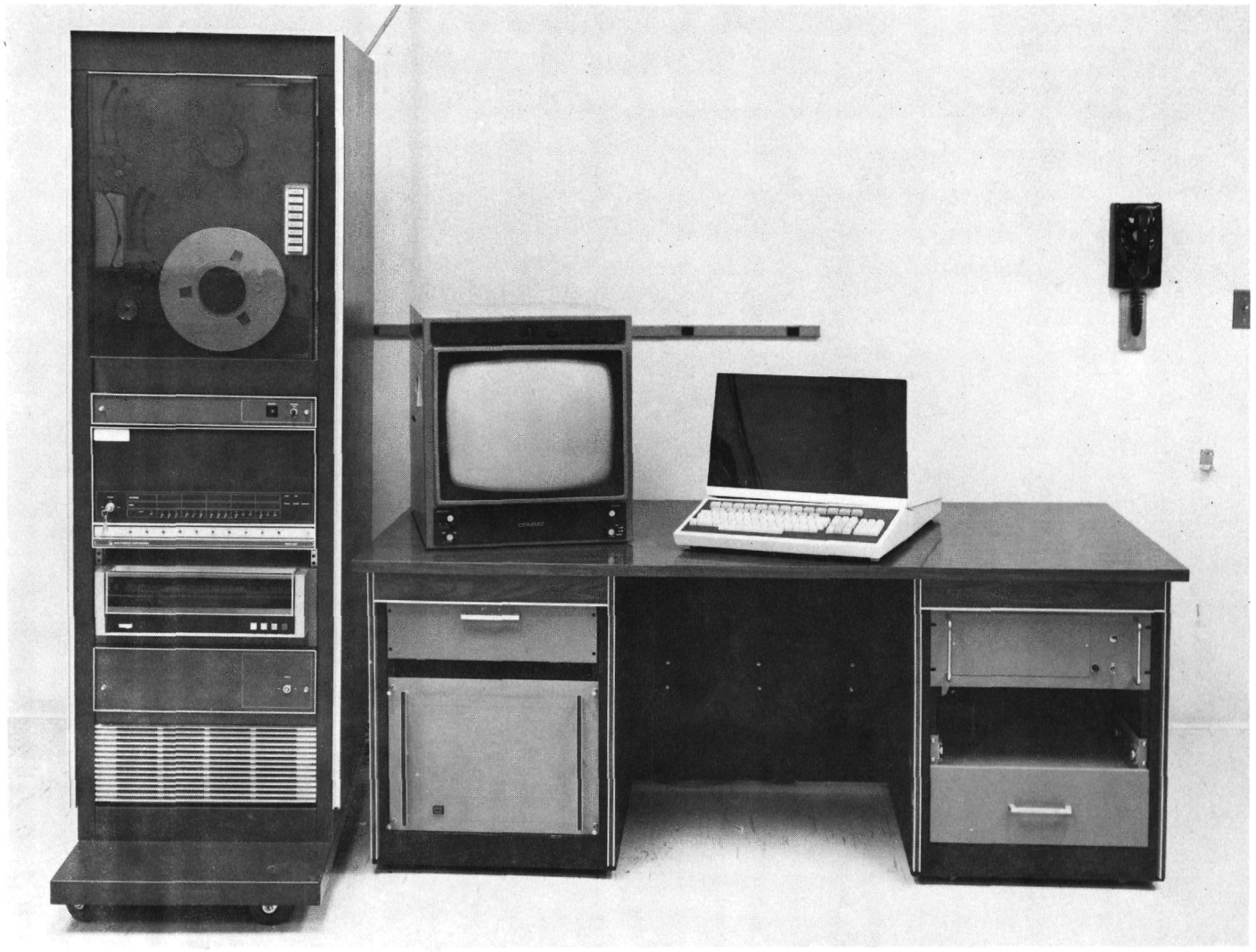

CY-077

Figure 4. Processing and Display Facility